INTERNATIONAL JOURNAL OF MULTIDISCIPLINARY RESEARCH AND ANALYSIS

ISSN(print): 2643-9840, ISSN(online): 2643-9875

Volume 08 Issue 09 September 2025

DOI: 10.47191/ijmra/v8-i09-31, Impact Factor: 8.266

Page No. 5189-5194

Plasmonic Color Filters Coupled with CMOS Photodetectors Integrated Within the Device

Kaesar Sabah Khalaf [1], Maroa Essam Baker[2]

[1,2]Technical Engineering College for Computer and Northern Technical University, Iraq

ABSTRACT: Modern, portable electronics employ CMOS image sensor arrays, which have tiny active pixels that are well-suited to the subwavelength mode volumes of plasmonic filters. Broad transmission bandwidths (> 100 nm) are characteristic of most plasmonic filters, making them ideal for CMYK or RBG color filtering. Achieving CMOS image sensors with multi- and hyperspectral imaging capabilities would be possible with a significant reduction in the peak width of filter transmission spectra. Single transmission bands as thin as 17 nm are produced by multi-mode interference phenomena, which are induced by the design of 4-layer metal-insulator-metal-insulator-metal structures. These phenomena reduce spurious transmission characteristics. The fundamental structure of these multilayer slot-mode plasmonic filters (MSPFs) may function across a wide range of wavelengths, allowing for systematic variation of the transmission peaks over the visible and near infrared spectra. This, in turn, produces a filter that can be integrated into complementary metal-oxide semiconductors (CMOS). We provide practical prototypes of MSPF filter designs that can attain a visible bandwidth of less than 30 nm and a full width at half maximum (FWHM) of 50 nm. We also detail how to make the experimental structure approach the limitations proposed by the model.

KEYWORDS: various semiconductors made of metal oxide, image sensors, optical filters.

I. INTRODUCTION

Image sensors that are based on CMOS are now the most used technology for digital imaging on the mass market. Over the course of the last ten years, the rate of feature.

The performance of single-pixel plasmonic complementary metal oxide image sensors has seen a tremendous increase as a consequence of the size reductions that have occurred in CMOS technology. The pixel size has seen a reduction from being more than 10 µm to being less than 2 µm [1]. On the other hand, now that the pixel size has been reduced to the sub- 2 µm region, the polarizer designs, standard filter and lens are seeing a decline in performance, which includes color crosstalk [2]. Dye-doped polymers are used in the color filtering methods that are now in use for CIS. The fabrication of each color filter for green , blue , and red must be carried out in a sequential manner throughout a number of process stages. It would be desired to discover new approaches to the construction of color filters into CIS. This is because the challenges of crosstalk are becoming more complex and the cost of manufacturing is increasing. Surface plasmon resonance (SPR) on thin metal films provides a candidate that is worthy of consideration for the production of filters [4]. When it comes to CIS, Catrysse and Wandell were the ones who first suggested the concept of employing SPR to create color filters [5]. Through the use of thorough numerical simulations and the provision of preliminary experimental data, they were able to demonstrate the potential of the technique [5–7-6]. The technology has the potential to make it possible to manufacture all of the necessary color filters on a single film by using the lesser metals that are often used in a typical CMOS process. As a result, this would result in a reduction in both cost and color crosstalk. For the time being, there have been very few demonstrations of the possibility for regulating light by utilizing metal on CMOS processors. In their study, David and colleagues proved that the SPR effect led to an increase in the photocurrent of a CMOS detector that had a nanoaperture in the form of a C [8]. In order to reduce the amount of infrared light that was present, Lee et al. included a visible passband filter that was constructed using aluminum gratings into a CIS [9]. It was established by Frey and colleagues that numerous Fabry–Perot (FP) cavities might be used for the purpose of color filtering on CIS [10]. The entire constructions, on the other hand, needed a significant number of manufacturing phases. The purpose of this letter is to show that color filters that are based on the Surface plasmon resonance phenomena may be manufactured and characterized using complementary metal oxide semiconductor photodiodes. The development of nanostructures in an aluminum film that was placed on top of the photodiode, which functions as a color filter, was accomplished by the use of electron beam lithography. A confirmation of the filtering response for the three main colors was obtained by the measurement of the photocurrent that was produced by the photodiodes. An further development of the technology might result in the creation of a plasmonic CIS pixel array. A lot of our lives have been changed by the 1969 development of semiconductor-based imaging, which was honored with the Nobel Prize in 2009, since it changed a lot of things. There are more cell phones in circulation than humans, and the majority of them include CMOS cameras. [1] Digital imagers are fundamental to the most cutting-edge tools that humanity has developed for investigating the cosmos and everything in it, from the tiniest particles to the largest galaxies. The bandgap of silicon, the solid-state imaging was used in first semiconductor, prohibits imaging with wavelengths above around 1 µm. the first infrared focal plane array based on indium bump-bonding was achieved, thanks to the requirement for imaging at longer wavelengths and the integration of diverse semiconductors on silicon. [2] in For the last fifty years, this integration technology has been the gold standard for heterogeneous semiconductor integration on silicon. The high price and low resolution of non-silicon imagers are caused by the impracticality of indium bump-bonding. The intrinsic features of epitaxially bulk produced semiconductors have hindered the success of considerable efforts in finding better integration techniques, such as DARPA's wafer size infrared detectors.

An exciting new nanowires and 2D van der Waal (vdW) materials are examples of low-dimensional materials that have recently emerged as a platform for imaging applications throughout the electromagnetic spectrum, from X-ray to terahertz (THz) frequencies. Finishing off the surface naturally free of dangling bonds, low capacitance, and flexibility are some of the distinctive physical characteristics of these materials. These characteristics provide a number of intriguing new possibilities that may influence the development of digital photography in the future, including the prospect of improved heterogeneous integration approaches. Imagers' spatial resolution, spectrum variety, and energy efficiency have all shown steady improvement over the years, as seen in Figure 1. Even if this statistic doesn't include all the crucial factors, it's clear that the technology has become much better at its core metrics thanks to a lot of commercial and research uses. Here we take a look at some of the ways that imaging could be revolutionized in the next decades by capitalizing on the special characteristics of low-dimensional materials. The following are the most significant implications, in our opinion:

1)Cameras that are both affordable and very effective in several electromagnetic bands: Low-cost solutions with similar or better performance than current cameras in problematic electromagnetic bands such as X-ray, deep ultraviolet (DUV), infrared (IR), and terahertz (THz) may be created by "stapping" vdW and 2D material on top of silicon circuitry (ROIC). At X-ray, DUV, IR, and THz, flexible detectors based on 2D material have previously been shown [3, 4, 5, 6, 7]. On the other hand, Eliminating the yield-limiting indium bump-bonding method opens the door to low-cost camera manufacture throughout a wide range of electromagnetic spectrum. In what follows, we demonstrate that, because to their intrinsic flexibility, they may be bonded to the non-planar surfaces of current or future ROICs manufactured by traditional CMOS fabs, bypassing the need for an intermediary material.

2)Surface passivation is unnecessary because vdW materials have atomically flat surfaces and few dangling bonds. [10] Because they are innately nanoscale, these materials are much simpler to deal with at smaller dimensions than traditional semiconductors, which need considerable surface passivation. Because of this quality, producing this material becomes easier, and it may be stacked to make sophisticated and/or multi-functional sensors.

3)Adaptations to new environments modeled after natural ones: the human eye has exceptional sensitivity, resolution, efficiency, and field of vision. Ganglion cells pre-process signals from the human eye's rod cells—which can detect a single photon—in an incredibly efficient and resilient manner before sending them on to the brain. A lot of work has gone into developing silicon-based devices that can replicate these kinds of natural sensors, but they still can't compare to the real thing in terms of performance. In our opinion, low-dimensional materials provide a once-in-a-lifetime chance to design imaging systems that are very similar to biological ones, allowing us to build a new generation of imaging systems with extraordinary capabilities like: a)Maximum photon sensitivity: it can be shown that the sensitivity of photodetectors, provided they have a sufficiently big internal gain, is dependent on their internal capacitance. Therefore, as shown experimentally, lowering the capacitance of these photodetectors may result in devices with increased sensitivity . As the capacitance of the device becomes closer to the quantum capacitance of $C0 = q2/kT$, where T is the temperature ,q is the electron charge, and k is the Boltzmann constant the sensitivity to a single photon becomes apparent. Because C0 is so tiny at ambient temperature, it is very difficult to fabricate room temperature single-photon detectors using top-down nano-fabrication techniques. Nevertheless, the ability to fabricate such devices using low-dimensional materials is intriguing because of their innately short dimensions and very low dielectric constants. b) Multi-band imaging: Beyond the visible band, scientists have achieved great strides in extending the spectral imaging range. The creation of cameras capable of detecting polarization in addition to more than three visible-light hues is an encouraging area of study. Scientists are investigating the possibility of creating synthetic versions of mantis shrimp—which possess polarization sensitivity and seven color sensors—to improve sensing and detection in many contexts. Even more advanced would be imaging in more than one spectral band at the same time, such visible, infrared, and THz. Such cameras have the potential to provide an unprecedented amount of data in a space-saving package. Because of their exceptional sensitivity to a broad spectrum of electromagnetic radiation (EMR), including X-rays, deep ultraviolet (DUV), infrared (IR), and transients (THz), low-dimensional materials are ideal for use in the development of multi-band cameras. It is within the realm of possibility to construct cameras capable of sensing several wavelength bands concurrently by integrating various two-dimensional materials. Numerous domains might benefit greatly from the use of such cameras, including astronomy, medical imaging, military, and remote sensing. c)Passive depth extraction: Jumping spiders (Salticidae) are able to properly produce a 3D depth picture because their retina is composed of layered transparent retinae. 2D materials provide a one-of-a-kind chance to create cameras with 3D depth sensing due to their thinness and stackability. More recently, integral imaging and depth awareness were enabled by semi-transparent 2D photodetectors. Effective, space-saving, and interference-free passive depth imaging techniques exist, in contrast to the conventional active ranging that relies on the emission of electromagnetic waves.

d)The retinae of advanced animals have a curved shape, which acts as an image sensor. Since curved focal plane arrays may decrease the size, complexity, and cost of the optics, it is not unexpected that they have a major benefit over flat ones . Particularly in the X-ray and DUV bands, where regular lenses fail, this becomes crucial. The good news is that a novel technique has been discovered that makes it possible to thin and shape any commercial silicon CMOS image sensor into an accurate, highly curved optical surface without compromising its performance. is a Cameras that need non-silicon material, such as those that are sensitive to infrared or other bands, cannot be made using this process since it is incompatible with indium bump-bonding. Although it has not been proven yet, we suggest that curved ROICs combined with 2D material might provide small, high-performance cameras that excel in demanding electromagnetic bands.

e)In-sensor computing: Along with photosensitive cone and rod cells, the human eye also has a separate group of cells called ganglion cells that do a lot of early processing. They work by drastically decreasing data volume while preserving event spatial and temporal resolution. Torstein Wiesel, who won the Nobel Prize in medicine in 1981, first shown that this accomplishment could be accomplished by suppressing undesirable spikes . Curiously, there is mounting evidence that low-dimensional materials are well-suited to neuromorphic computing that requires less energy. The medical, high-energy particle physics, and astronomical communities would all benefit greatly from in-sensor computing, also known as "in-pixel computing," which would allow for images with very high resolution and little power usage.

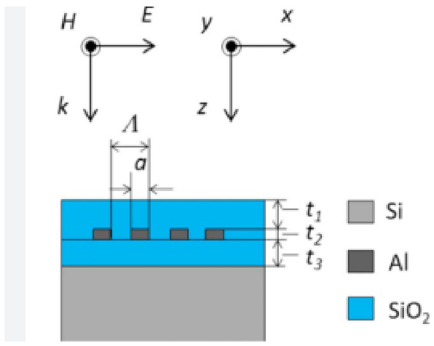

Fig 1 A Photodiode Array That Has Color Filters Integrated

II. CHARACTERIZATION AND FABRICATION OF THE PARTS

Among the requirements necessary to accomplish color filtering in plasmonic CIS, Surface plasmon resonance is the most essential need. Both two dimensional and one dimensional subwavelength structures have been shown to be capable of being used in order to stimulate surface plasmon resonance (SPR) and accomplish color filtering [10], [11]. in an aluminum film that was evaporated onto a piece of glass microscope slide was the method that was used in this work to show complete color control utilizing surface plasmon resonance (SPR) in a two-dimensional hole array application. In order to produce the nanostructures, a technique that included dry etching and single electron beam lithography was used. An extra cap layer of silicon dioxide was placed on the top surface in order to achieve optimal performance of the transfer function [8]. For the purpose of analyzing the SPR color picture that was produced, an Olympus BX51 microscope that was equipped with a broadband Halogen light was used. The university logo was noticed to have a hue that was well defined, as seen in Figure 2(a). An picture captured by a scanning electron microscope (SEM) of the portion of the logo that defines the bird is shown in Figure 2(b). As illustrated in Figure 1(b), the nanostructures that are present in the aluminum film change depending on the color section that is being considered. Using a single lithographic process, it is possible to produce a variety of color filters in a reliable manner. Despite the fact that features as tiny as 1 μm still display strong color differentiation, this approach demonstrates the possibility for this technology to be used for sub-μm CIS.

Plasmonic Color Filters Coupled with CMOS Photodetectors Integrated Within the Device

A single-pixel photodiode, made using a 0.18 µm process by United Microelectronics Corporation (UMC), is installed in the CIS that was used in this particular scientific endeavor.

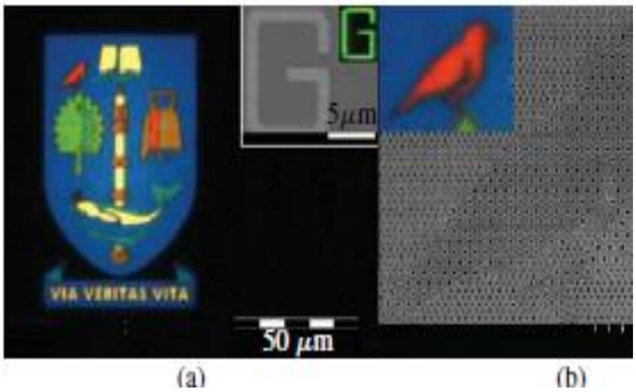

Fig2. captured in full color plasmonic pictures using the transmission mode of the microscope.

In the inset, there is a patterned letter "G" that indicates the color green with a line that is one micrometer broad. (a) A scanning electron micrograph showing a portion of the produced logo with the pattern. These magnified pictures from the microscope are shown in the inset.

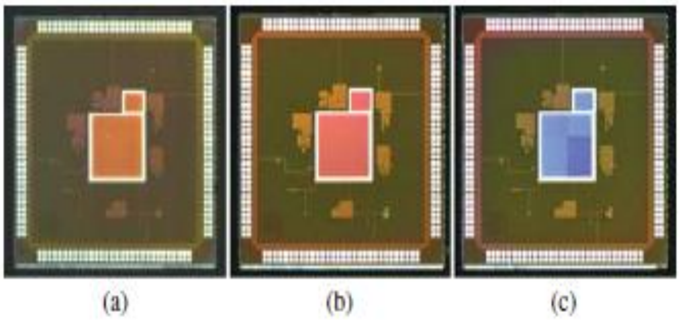

Fig 3 Images of CIS captured by a microscope equipped with (S1) blue, (S2green), and (S3) red plasmonic color filters incorporated into the picture.

must be altered from the method that was used in [11] for the production of plasmonic filters on glass. After depositing a layer of SiNx on top of the Snil surface passivation layer of the Snix, we proceeded to install a 160 nm film of aluminum using evaporation. This was done in order to enhance the transmission of the color filters that were integrated on the CIS. It was also the bond pads of the chip that were protected by this SiNl layer while it was being processed. Before spin-coating the aluminum film with ZTRE20K electron beam resist, a small layer of Snil was applied to the film in order to promote adhesion. An electron beam lithography instrument called a Vistec VB6 UHR EWF was used in order to expose the sample. A sample was etched using CHF3 and Ar in a Plasmalab 89 plus, and then it was etched using SiCl4 in a Plasma System 100. This was done after the sample had been developed in o-xylene beforehand. Following the deposition of a Snil cap layer with a thickness of 200 nanometers, an additional mask and etch step was necessary in order to reopen windows that were located above the bond pads of the integrated circuits. While the chip was being processed, it was attached to a silicon carrier in order to facilitate handling. The pictures of the processed CIS that were captured by the reflection microscope revealed a variety of colors for the pixels, as can be seen in Figure 2(a)–(c)., green (sample S2), Blue (sample S1) and red (sample S3) light were intended to pass through the three major color filters that were integrated on the CIS shown in Figure 2(a)–(c). These filters were designed to allow light to reach the photodiodes.

Consequently, the reflection spectra demonstrated a complementary minimum in the reflection coefficient for each color filter. This was in conformity with the previous statement. In addition, we can see a color fluctuation that is present over the whole photodiode region in Figure 2(c). The production of the nanohole array involves non-uniformity, which is the source of this phenomenon. This non-uniformity occurred as a result of the CIS being bound to a carrier by the use of photoresist, as well as the presence of a tilt error that was not insignificant during the electron beam lithography process. Within the broad pixel region, as can be seen in Figure 3(c), there are four little areas that are somewhat different in color from one another. The limits of the electron beam writing fields, as well as the boundaries between the various sections, are the boundaries between which there is the biggest differences.

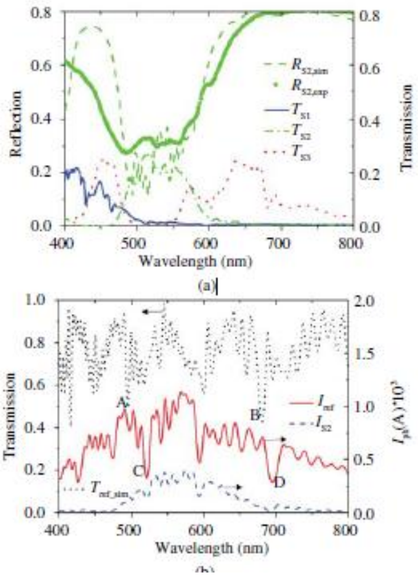

Fig4 . (a) as well as the observed reflection spectra of S2. (b) The reference as well as S2 photocurrents as measured.

at the production scale of wafers. Figure 3(a) displays the simulated transmission spectra of each of the three samples. In order to recreate the CIS structure, a whole stack of layers was modeled using the finite-difference time-domain approach. The design data of the UMC 0.18 µm process was used to calculate the stack parameters. Sections 1, 2, and 3 each have periods and radiuses of 250 nm and 80 nm, 340 nm and 90 nm, and 420 nm and 110 nm, respectively. We measured the reflection spectrum instead of the transmission spectra on the CIS since we couldn't get the former to work. Figure 3(a) displays the outcome for sample S2. Clearly, there is a high degree of agreement between the experimental and simulation outcomes. The experimental data show a little broader minimum in the reflection coefficient compared to the modeling. The key reason behind this is

Table 1 COLOR CROSSTALK

Blue 400-495 nm	Red 200-250 nm	Green 300-400nm	Color %
14	17	25	14
20	22	29	27
19	12	18	17

due to the previously mentioned non-uniformity of the nanostructures across the 1 mm2 photodiode region. The CMOS photodiodes' photocurrents were measured with a tungsten an Agilent/HP 4155B, a monochromator, and two light bulbs. It was the monochromator's grating and slit that established the 5 nm experimental wavelength resolution. For a single sample, we ran 15 iterations of the scan to check for electrical and mechanical differences in the photocurrent meter and monochromator; we found nothing. Figure 4(b)'s red dash line reveals substantial changes in the photocurrent spectra of an unprocessed reference CIS, with two prominent dips labeled C (520 nm) and D (695 nm) standing out. Figure 4(b) shows that the experimental dips are quite close to the simulated dips A and B, which were obtained by a basic transfer matrix technique simulation of the whole dielectrics stack. Rooted in the CIS dielectric stack, the dips are caused by FP resonances. As is common for commercial CIS, this outcome is not surprising given that the CMOS technology we used has not been optimized. Due to the impossibility of directly measuring the transmission spectrum, we have calculated the relative transmission by making a comparison between the photocurrent of sample S2 and that of a reference CIS that has not been treated. When looking at the relative transmission spectra of S2 in Figure 3(b), one can see an apparent green transmission band that has an average transmission of around thirty percent and a full-width at half-maximum of one hundred thirty nanometers. Strong transmission peak at 750 nm is the consequence of the displacement of the labeled dip D in the photocurrent of S2 as a result of the change in the stack dielectric structure obtained by our processing in comparison to the reference CIS. This change is caused by the differences between the two structures. This unwanted dip would be eliminated if the CIS dielectric stack were put through the optimization process. As may be seen in Figure 4(b), the transmission of CIS S3, S2, and S1 is described. There is a clear visualization of the blue, green, and red transmission bands.

Plasmonic Color Filters Coupled with CMOS Photodetectors Integrated Within the Device

Figure 4(a) shows the findings of the simulation, however these bands are broader. We believe that the fluctuating manufacturing tolerance for the necessary hole sizes and the overall nonuniformity of the nanostructures across the photodiode region are to blame for the poor performance. Also, the undesirable F and G transmission peaks in the less-than-ideal configuration are due to FP resonances. FP resonances in the unoptimized layer stack also cause the undesired transmission peaks labeled F and G., the color crosstalk was assessed using the same methodology as a standard CIS. Table I shows that since the manufactured color filters have broader passbands, our plasmonic CMOS photodetectors experience increased crosstalk. However, with optimization of the production process and plasmonic filters, these may be minimized. Because the devices being examined here are single-pixel photodetectors, the computation does not take into account the fact that plasmonic color filters integrated into a CIS would decrease the color crosstalk between neighboring pixels.

III. CONCLUSIONS

As an alternative to the conventional pigment dye filters that are used in commercial CIS, we have shown a single-sensor CMOS photodetector that is equipped with plasmonic color filters. For the purpose of our inquiry into plasmonic color selectivity, we have used back-end-of-line processing methods such as electron beam lithography and dry etching. These CIS-integrated plasmonic color filters were shown to perform well, as indicated by the results of photocurrent measurements and experimental reflection spectra. It is anticipated that the half-pitch in Metal 1 will decrease to 32 nm in the year 202025, as stated in the ITRS road plan from 2024. This will make it feasible to mass-produce suitable SPR structures, which will be made possible by future CMOS technology that includes the most advanced technology. Therefore, without the need of multilayer processing of dye-based filters, this work may result in the development of enhanced CIS that has a lower cost and minimum crosstalk while also reducing the amount of crosstalk.

REFERENCES

1) Chen, Q., Das, D., Chitnis, D., Walls, K., Drysdale, T. D., Collins, S., & Cumming, D. R. S. (2012). A CMOS image sensor integrated with plasmonic colour filters. Plasmonics, 7(4), 695-699.
2) Itonaga, K., Arimura, T., Matsumoto, K., Kondo, G., Terahata, K., Makimoto, S., ... & Hirayama, T. (2014, June). A novel curved CMOS image sensor integrated with imaging system. In 2014 Symposium on VLSI Technology (VLSI-Technology): Digest of Technical Papers (pp. 1-2). IEEE.
3) Gouveia, L. C. P., & Choubey, B. (2016). Advances on CMOS image sensors. Sensor review, 36(3), 231-239.
4) Zhang, M., & Bermak, A. (2010). CMOS Image Sensor with On-Chip Image Compression: A Review and Performance Analysis. Journal of Sensors, 2010(1), 920693.
5) Goossens, S., Navickaite, G., Monasterio, C., Gupta, S., Piqueras, J. J., Pérez, R., ... & Koppens, F. (2017). Broadband image sensor array based on graphene–CMOS integration. Nature Photonics, 11(6), 366-371.
6) Mendis, S. K., Kemeny, S. E., Gee, R. C., Pain, B., Staller, C. O., Kim, Q., & Fossum, E. R. (1997). CMOS active pixel image sensors for highly integrated imaging systems. IEEE Journal of Solid-State Circuits, 32(2), 187-197.
7) Skorka, O., & Joseph, D. (2011). Design and fabrication of vertically-integrated CMOS image sensors. Sensors, 11(5), 4512-4538.
8) Stoppa, D., Simoni, A., Gonzo, L., Gottardi, M., & Dalla Betta, G. F. (2002). Novel CMOS image sensor with a 132-dB dynamic range. IEEE Journal of Solid-State Circuits, 37(12), 1846-1852.
9) Carlson, B. S. (2002, June). Comparison of modern CCD and CMOS image sensor technologies and systems for low resolution imaging. In SENSORS, 2002 IEEE (Vol. 1, pp. 171-176). IEEE.
10) Schanz, M., Nitta, C., Bußmann, A., Hosticka, B. J., & Wertheimer, R. K. (2002). A high-dynamic-range CMOS image sensor for automotive applications. IEEE Journal of Solid-State Circuits, 35(7), 932-938.
11) Gow, R. D., Renshaw, D., Findlater, K., Grant, L., McLeod, S. J., Hart, J., & Nicol, R. L. (2007). A comprehensive tool for modeling CMOS image-sensor-noise performance. IEEE Transactions on Electron Devices, 54(6), 1321-1329.